Low Temperature Physics/Fizika Nizkikh Temperatur, 2016, v. 42, No. 7, pp. 760–763

Cathodoluminescence characterization of polystyrene–$BaZrO_3$ hybrid composites

V.P. Savchyn[1], A.I. Popov[2], O.I. Aksimentyeva[1], H. Klym[3], Yu.Yu. Horbenko[1], V. Serga[4], A. Moskina[2], and I. Karbovnyk[1]

[1]*Ivan Franko National University of Lviv, Ukraine*

[2]*Institute of Solid State Physics, University of Latvia, Riga, Latvia*
E-mail: popov@latnet.lv

[3]*Lviv Polytechnic National University, Ukraine*

[4]*Institute of Inorganic Chemistry, Riga Technical University, Latvia*

Received April 6, 2016, published online May 25, 2016

The radiation properties and the electronic structure of hybrid composites based on suspension polystyrene (PS) and nanocrystals of $BaZrO_3$ (BZO) (d < 50 nm) have been studied using luminescent spectroscopy and x-ray analysis. A strong cathodoluminescence (CL) in BZO-nanocrystals is observed in temperature range 80–293 K. It is modified in BZO–PS composites: both the low- and a high-energy bands (near 4 eV) appear, together with a significant reduction in the CL intensity. A decrease of the lattice parameter a for BZO phase in the composite and the modification of CL spectra indicate for changes in the nanocrystalline structure induced by the polymer.

PACS: **78.47.–p** Spectroscopy of solid state dynamics;
78.55.–m Photoluminescence, properties and materials.

Keywords: $BaZrO_3$ powders, cathodoluminescence spectroscopy, hybrid composite, polystyrene.

1. Introduction

Inorganic/organic nanosystems based on semiconductor nanocrystals and conducting or thermoplastic polymers such as polymethylmetacrylate and polystyrene are prospective for a number of applications and thus nowadays attract much attention [1–4]. These polymers are useful for optical devices due to their transparency in the visible range of the spectrum and relatively high stability. For the preparation of polymer–semiconductor nanocomposites, the semiconducting nanocrystals of CdTe, CdSe, ZnS, CdS are mainly used. At the same time, different physical properties of oxide materials, including oxide perovskites, suggest obtaining hybrid materials with new completely different functional characteristics.

$BaZrO_3$ (BZO) perovskite has found several applications, such as substrate for the synthesis of superconductors, high-temperature microwave dielectrics, electrolyte for protonic fuel cells [5–15]. Since recently it also attracts a considerable attention as a fluorescent material. It is well known that the luminescent characteristics of BZO significantly depend on fabrication technology of micro- and nanocrystals; using different technological routes, samples can be tailored to show violet, blue, green or red luminescence [7,8,16–20].

In the present work, we studied the effect of polymer matrix on the luminescent properties and the structure of hybrid composites based on BZO nano- and microcrystals embedded in the polystyrene (PS) matrix using cathodoluminescence (CL) spectroscopy and XRD analysis.

2. Experimental

2.1. Materials and compounds

Commercial BZO powders (grain size d < 50 nm and d < 10 μm) from ALDRICH company were used for the preparation of BZO–polystyrene hybrid composites.

Polystyrene was synthesized by suspension polymerization of styrene (St) in the presence of peroxide initiators of polymerization–benzoyl peroxide and ammonium persulphate $(NH_4)_2S_2O_8$ and starch as suspension stabilizer at the temperature of 60 °C.

Samples were prepared by sonification of 7–40 mg of BZO nano- or micropowders in the 1% solution of toluene sulfonic acid used as surfactant during 60 min. The obtained nanodispersions were added to solution of PS in toluene and sonoficated during 10 min to obtain the uniform dispersion. For solvent evolution the samples were dried in dynamic vacuum at 60 °C during 6–8 h to constant mass. All investigated samples were prepared as pellets.

2.2. Measurements

The cathodoluminescence excitation was performed by a pulse-mode electron gun (the beam energy of 10 keV at current of 100 μA, pulse duration of 2 μs at the frequency of 300 Hz). The luminescence spectra were recorded in the energy range of 1.0–5.0 eV at room temperature (RT) and liquid nitrogen temperature (LNT). This experimental set-up is an unique tool for the in-situ investigations of the electronic structure of wide band gap materials as well as of nanocrystalline semiconductors [21–25].

The x-ray powder diffraction data were collected on the automated diffractometer STOE STADI P with a linear PSD detector (transmission mode; Cu $K_{\alpha 1}$ radiation, a curved germanium (111) monochromator).

3. Results and discussion

3.1. CL characteristics of initial BZO powders

The CL spectrum of nano-BZO ($d < 50$ nm) pellet at RT is shown in Fig. 1 (curve *1*). The respective Gaussian decomposition into three possible bands *A*, *B*, *C* is also presented. This spectrum is similar to PL emission profile [16,17] and is typical for multiphonon and multilevel process, *i.e.*, a system in which the electronic relaxation occurs by several paths, including numerous energy levels within the band gap [7]. According to [16–20,26], this behavior is related to the structural disorder of BZO including $[ZrO_5 \cdot V_O^*]$–$[ZrO_6]$ complex clusters.

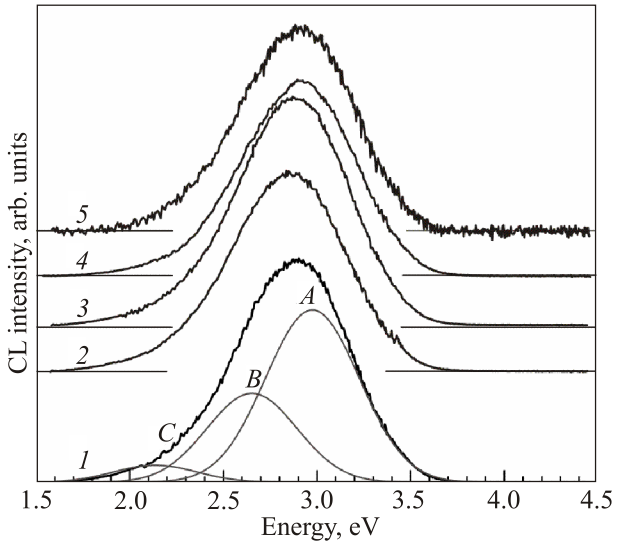

Fig. 1. CL spectra at RT of nano-BZO pellets: *1* — as prepared (with Gaussian decomposition), *2–5* — annealing during 2 h at 400, 500, 700 and 800 °C, respectively.

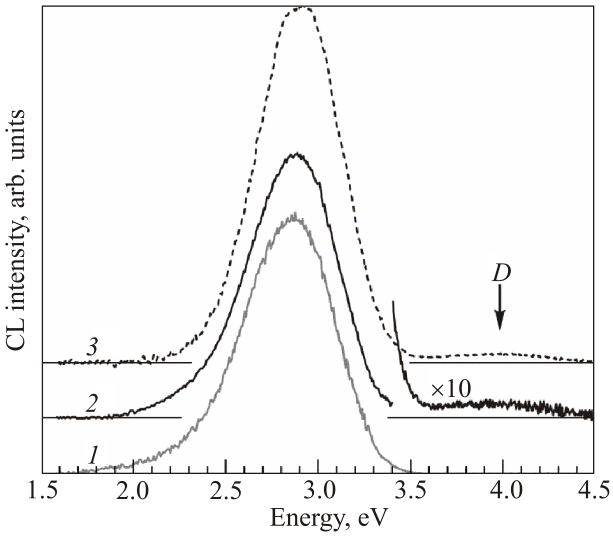

Fig. 2. CL spectra at LNT of nano-BZO pellets (*1* — as prepared, *2* — annealing during 2 h at 800 °C) and micro-BZO pellets (*3*).

Figure 2 illustrates CL spectra of nano-BZO samples, both as prepared and annealed during 2 h at different temperatures (up to 800 °C). These results demonstrate high-temperature stability of CL intensity and spectral composition, contrary to the results published earlier [16–20,26]. This behavior is attributed to micro-BZO ($d < 10$ μm) powders.

As is shown in Fig. 2, the high-energy band *D* (near 4 eV) for as prepared micro-BZO pellets (curve *3*) is observed only at LNT. For nano-BZO pellets, however, the weak band *D* appears only after high-temperature annealing (curve *2*). We believe that this could be caused by the surface-related defects. It is known such near band gap emission in $BaZrO_3$ strongly depends on the conditions of fabrication and structural quality of samples [16,18,27].

3.2. Structure characterization

The x-ray powder diffraction pattern for BZO nanocrystals (Fig. 3, curve *1*) shows the crystalline structure of BZ powders, it is typical for nanosized BZO powder described in literature [18,19,27]. A small amount of $BaCO_3$ phase is observed, which can be expected for such samples [18,19,27]. By means of XRD analysis it is found that BZO exhibits a cubic perovskite-type structure, in the crystalline form with the space group *Pm*-3*m*. The BZO lattice parameter at RT $a = 4.19083(6)$ Å with the average size of domains 23 nm.

In a polymer, only one amorphous halo is developed on the XRD pattern (Fig. 3, curve *2*) with a maximum at $2\theta = 19.53°$; the average apparent size of domain is here 13.16 Å.

Lastly, in the BZO–PS composite a coexistence of amorphous halo with the diffraction peaks of BZO (Fig. 3, curve *3*)

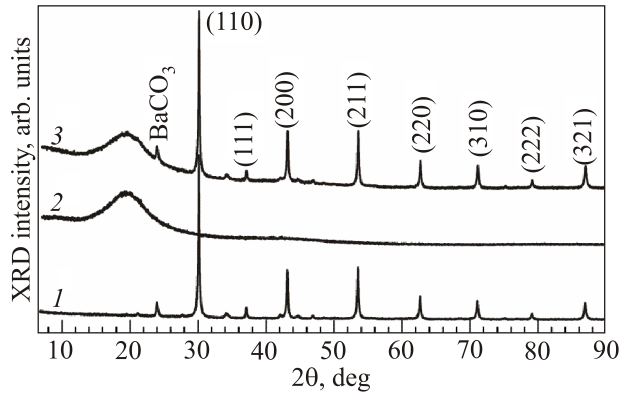

Fig. 3. The x-ray powder diffraction pattern for BZO nanocrystals (*1*), PS matrix (*2*) and BZO–PS composite (*3*).

is observed, which is a clear evidence for the nanocomposite formation. The BZO lattice parameter decreases down to a = 4.1879(2) Å, both microstructural parameters remain practically unchanged. It is suggested that polystyrene significantly alters the subsurface structure of BZO, indicating the formation of fractal aggregates and structures.

3.3. CL data of PS-BZO composites

The PS–BZO composites show the modification of the CL spectrum. The Gaussian decomposition of CL curves shows that the additional lowest energy band *E* and the highest energy band *D* (near 4 eV) arise, accompanied with a significant reduction in the CL intensity. As seen from a comparison of CL spectra of BZO–PS composites with nano-BZO (Fig. 4(a)) and micro-BZO (Fig. 4(b)), the ratio between the intensities of the lower energy CL bands and higher ones strongly depends on the BZO grain size.

These changes of CL spectra could be caused by the BZO grain changes caused by the polystyrene. In particular, the polystyrene reacts with BZO, creating structural changes that lead to the additional CL bands (*D* and *E*), a relative increase in the intensity of band *C* and the decrease in the intensity of *A* band. Moreover, such structural changes occur only in the subsurface layer of BZO grains, as it is demonstrated by a comparison of Fig. 4(a) and (b). We suggest that polystyrene molecules create weak covalent bonds with oxygen vacancies of BZO nanocrystals, accompanied with the formation of intermediate defect complexes, which induce new energy levels in the band gap.

5. Conclusions

Polystyrene significantly alters the subsurface BZO structure due to the formation of hybrid nanocomposite. The decrease of the lattice parameter from a = 4.19083(6) Å in nano-BZO to 4.1879(2) Å in the BZO–PS composite, the modification of the CL spectra for BZO–PS (appearance of low- and a high-energy band (near 4 eV)) and a significant reduction of the CL intensity, all indicate a notable change in the BZO structure caused by the polymer.

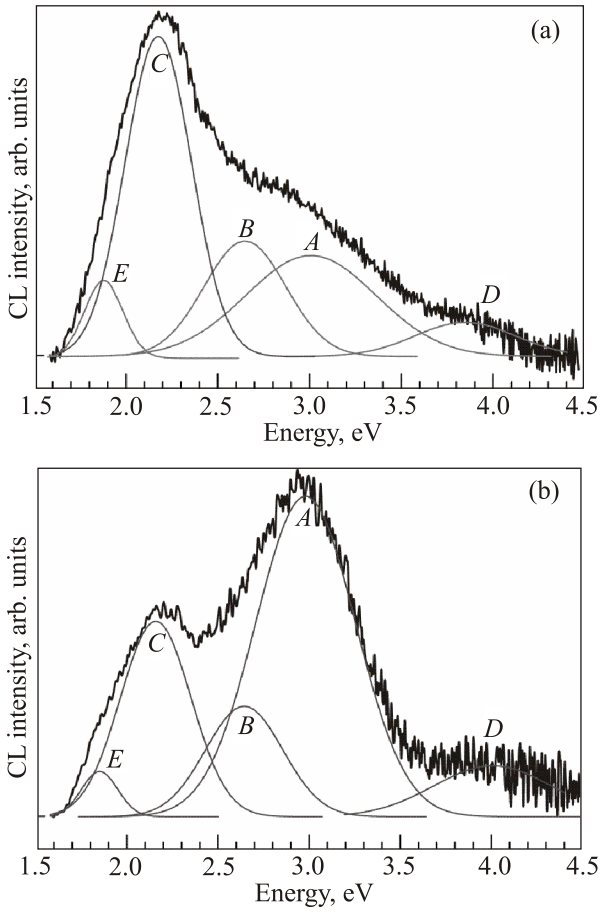

Fig. 4. CL spectra of nano-BZO–PS (a) and micro-BZO–PS (b) composite at RT.

Acknowledgments

A.I. Popov and A. Moskina would like to thank the support of State research program IMIS2, while H. Klym was supported by the Lviv Polytechnic University under Doctoral Program and support via the Project DB/KIBER (No. 0115U000446).

1. M.J. Panzer, K.E. Aidala, and V. Bulović, *Nano Rev.* **3**, 16144 (2012).
2. Y. Yang, Z. Wen, Y. Dong, and M. Gao, *Small* **2**, 898 (2006).
3. M. Tamborra, M. Striccoli, R. Comparelli, M.L. Curri, A. Petrella, and A. Agostiano, *Nanotechnol.* **15**, S240 (2004).
4. J.Q. Liu, X.Y. Qi, T. Jiang, Z.Q. Lin, S.F. Chen, L.H. Xie, Q.L. Fan, Q.D. Ling, H. Zhang, and W. Huang, *Sci. China Chem.* **53**, 2324 (2010).
5. K.D. Kreuer, S. Adams, W. Munch, A. Fuchs, U. Klock, and J. Maier, *Solid State Ionics* **145**, 295 (2001).
6. H. Iwahara, T. Yajima, T. Hibino, K. Ozaki, and H. Suzuki, *Solid State Ionics* **61**, 65 (1993).
7. O.I. Aksimentyeva, V.P. Savchyn, V.P. Dyakonov, S. Piechota, Y.Y. Horbenko, I.Y. Opainych, P.Y. Demchenko, A. Popov, and H. Szymczak, *Mol. Cryst. Liq. Cryst.* **590**, 35 (2014).

8. O. Aksimentyeva, V. Savchyn, I. Opaynych, P. Demchenko, Y. Horbenko, V. Pankratov, and A.I. Popov, *Chem. Metall. Alloys* **6**, 177 (2013).
9. T.S. Bjørheim, M. Arrigoni, D. Gryaznov, E. Kotomin, and J. Maier, *Phys. Chem. Chem. Phys.* **17**, 20765 (2015).
10. M. Arrigoni, E. Kotomin, D. Gryaznov, and J. Maier, *Phys. Status Solidi (b)* **252**(1), 139 (2015).
11. T.S. Bjørheim, M. Arrigoni, S.W. Saeed, E.A. Kotomin, and J. Maier, *Chem. Mater.* **28**, 1363 (2016).
12. T.S. Bjorheim, E.A. Kotomin, and J. Maier, *J. Mater. Chem. A* **3**, 7639 (2015).
13. R.I. Eglitis, *Int. J. Mod. Phys. B* **28**, 1430009 (2014).
14. R.I. Eglitis, *Solid State Ionics* **230**, 43 (2013).
15. R.I. Eglitis, *J. Phys.: Condens. Matter* **19**, 356 (2007).
16. L.S. Cavalcante, J.C. Sczancoski, V.M. Longo, F.S. De Vicente, J.R. Sambrano, A.T. de Figueiredo, C.J. Dalmaschio, M. Siu Li, J.A. Varela, and E. Longo, *Optics Commun.* **281**, 3715 (2008).
17. L.S. Cavalcante, V.M. Longo, M. Zampieri, J.W.M. Espinosa, P.S. Pizani, J.R. Sambrano, J.A. Varela, E. Longo, M.L. Simoes, C.A. Paskocimas, *J. Appl. Phys.* **103**, 063527 (2008).
18. L.S.Cavalcante, J.C.Sczancoski, J.W.M. Espinosa, V.R. Mastelaro, A. Michalowicz, P.S. Pizani, F.S. De Vicente, M.S. Li, J.A. Varela, E. Longo, *J. Alloys and Compounds* **471**, 253 (2009).
19. L.R. Macario, M.L. Moreira, J. Andrés, and E. Longo, *Cryst. Eng. Comm.* **12**, 3612 (2010).
20. M.L.Moreira, J.Andres, V.R. Mastelaro, J.A. Varela, E. Longo, *Cryst. Eng. Comm.* **13**(19), 5818 (2011).
21. A.I. Popov, *Opt. Spektrosc.* **65**, 1389 (1988).
22. A.I. Popov, S.A. Chernov, and L.E. Trinkler, *Nucl. Instrum. Methods B* **122**, 602 (1997).
23. S. Bellucci, A.I. Popov, C. Balasubramanian, G. Cinque, A. Marcelli, I. Karbovnyk, V. Savchyn, and N. Krutyak, *Radiat. Meas.* **42**, 708 (2007).
24. A. Huczko, A. Dąbrowska, V. Savchyn, A.I. Popov, I. Karbovnyk, *Phys. Status Solidi (b)* **246**, 2806 (2009).
25. V. Savchyn, I. Karbovnyk, A.I. Popov, A. Huczko, *Acta Physica Polonica A* **116**, s142 (2009). WOS: 000274113400041
26. S. Parida, S.K. Rout, L.S. Cavalcante, E. Sinha, M. Siu Li, V. Subramanian, N. Gupta, V.R. Gupta, J.A. Varela, and E. Longo, *Ceramics Intern.* **38**, 2129 (2012).
27. M.L. Moreira, J. Andres, J.A. Varela, and E. Longo, *Cryst. Growth Design.* **9**, 833 (2009).